



## ORIGINAL ARTICLE

# Miconazole inhibits signal transducer and activator of transcription 3 signaling by preventing its interaction with DNA damage-induced apoptosis suppressor

Sung-Hoon Yoon<sup>1,2,3</sup> | Bo-Kyung Kim<sup>1</sup> | Mi-Jung Kang<sup>1</sup> | Joo-Young Im<sup>1</sup>  | Misun Won<sup>1,4</sup> 

<sup>1</sup>Personalized Genomic Medicine Research Center, KRIBB, Daejeon, Korea

<sup>2</sup>National Center for Efficacy Evaluation for Respiratory Disease Product, Korea Institute of Toxicology, Jeongeup, Korea

<sup>3</sup>Department of Human and Environmental Toxicology, Korea University of Science and Technology (UST), Daejeon, Korea

<sup>4</sup>Department of Functional Genomics, KRIBB School of Bioscience, Korea University of Science and Technology (UST), Daejeon, Korea

## Correspondence

Misun Won and Joo-Young Im, Personalized Genomic Research Center, KRIBB, 125 Kwahag-ro, Yuseong-gu, Daejeon 34141, Korea.  
Emails: misun@kribb.re.kr and imjy@kribb.re.kr

## Funding information

Korea Research Institute of Bioscience and Biotechnology, Grant/Award Number: KGM4751713; National Research Foundation of Korea, Grant/Award Number: NRF-2015M3A9A8032460, NRF-2017M3A9F9030565 and NRF-2017R1A2B2011936

## Abstract

DNA damage-induced apoptosis suppressor (DDIAS) facilitates the survival of lung cancer by suppressing apoptosis. Moreover, DDIAS promotes tyrosine phosphorylation of signal transducer and activator of transcription 3 (STAT3) via their interaction. Here, we identified miconazole as an inhibitor of DDIAS/STAT3 interaction by screening a chemical library using a yeast two-hybrid assay. Miconazole inhibited growth, migration and invasion of lung cancer cells. Furthermore, miconazole suppressed STAT3 tyrosine Y705 phosphorylation and the expression of its target genes, such as cyclin D1, survivin and snail but had no suppressive effect on the activation of ERK1/2 or AKT, which is involved in the survival of lung cancer. As expected, no interaction between DDIAS and STAT3 occurred in the presence of miconazole, as confirmed by immunoprecipitation assays. Mouse xenograft experiments showed that miconazole significantly suppressed both tumor size and weight in an NCI-H1703 mouse model. Tyrosine phosphorylation of STAT3 at Y705 and expression of its targets, such as cyclin D1, survivin and snail, were decreased in miconazole-treated tumor tissues, as compared with those in vehicle-treated tumor tissues. These data suggest that miconazole exerts an anti-cancer effect by suppressing STAT3 activation through inhibiting DDIAS/STAT3 binding.

## KEYWORDS

DDIAS, lung cancer, miconazole, STAT3, yeast two-hybrid

## 1 | INTRODUCTION

Signal transducer and activator of transcription 3 (STAT3) is a well-known transcription factor, which is transiently activated by extracellular ligands such as growth factors or cytokines.<sup>1,2</sup> STAT3 regulates the expression of genes related to cell survival, proliferation and immune

response.<sup>3-5</sup> STAT3 is activated through the phosphorylation of STAT3 on tyrosine 705, which induces its dimerization, nuclear translocation and transcriptional activation.<sup>6,7</sup> However, constitutive STAT3 activation is ubiquitous in many human cancers, and aberrant activation of STAT3 is associated with malignant cancers with poor clinical prognosis, suggesting STAT3 as a potential target for cancer therapy.<sup>8,9</sup>

This is an open access article under the terms of the Creative Commons Attribution-NonCommercial License, which permits use, distribution and reproduction in any medium, provided the original work is properly cited and is not used for commercial purposes.

© 2020 The Authors. *Cancer Science* published by John Wiley & Sons Australia, Ltd on behalf of Japanese Cancer Association.

DNA damage-induced apoptosis suppressor (DDIAS) is highly expressed in lung cancer and hepatocellular carcinoma (HCC)<sup>10,11</sup> and is induced by the transcription factor nuclear factor of activated T cells 1 (NFATc1).<sup>12</sup> Moreover, DDIAS expression is induced by the extracellular signal-regulated kinase 5 (ERK5)/myocyte enhancer factor 2B (MEF2B) pathway in the presence of epidermal growth factor.<sup>13</sup> Moreover, DDIAS is ubiquitinated and degraded by E3 U-box ubiquitin ligase carboxyl terminus of heat shock protein 70-interacting protein (CHIP).<sup>14</sup> DDIAS promotes proliferation and colony formation and is involved in chemoresistance toward drugs such as cisplatin and camptothecin, and in tumor necrosis factor-related apoptosis-inducing ligand (TRAIL) resistance in lung cancer.<sup>10,13,15</sup> Interestingly, elevated DDIAS positively regulates cancer cell invasion by stabilizing  $\beta$ -catenin. Furthermore, DDIAS acts as a cofactor of DNA polymerase-primase complex through associating with DNA polymerase to promote tumorigenesis in HCC.<sup>11</sup> Recently, we reported that DDIAS functions as a positive regulator of signal transducer and activator of transcription 3 (STAT3) through physically associating with STAT3 to prevent its recruitment to protein tyrosine phosphatase receptor type M (PTPRM), sustaining the phosphorylation of STAT3.<sup>16</sup>

Miconazole (MIC), an antifungal agent, inhibits the enzyme cytochrome P450 14 $\alpha$ -demethylase, resulting in inhibition of fungal membrane ergosterol synthesis.<sup>17</sup> MIC also suppresses oxidative and peroxidative enzymes, leading to increased intracellular reactive oxygen species.<sup>18</sup> The anti-tumor activity of MIC has been demonstrated in human colon carcinoma, bladder cancer, osteosarcoma, breast cancer and glioma.<sup>19-21</sup> It induces apoptosis and G0/G1 cell cycle arrest in human colon carcinoma and inhibits the proliferation of osteosarcoma cells by increasing intracellular calcium levels by inducing calcium release from the endoplasmic reticulum.<sup>19,22</sup> Furthermore, MIC inhibits the mTOR pathway and induces phosphorylation of the translation initiation factor 2a (eIF2a), thereby suppressing HIF-1a protein synthesis.<sup>20</sup> MIC is reported to induce apoptosis through the death receptor 5-dependent and mitochondrial-mediated pathways in human bladder cancer cells.<sup>21</sup> Therefore, the anti-cancer effects of MIC are exerted via multiple pathways.

In this study, we demonstrate that MIC is an inhibitor of the interaction between DDIAS and STAT3, leading to suppression of STAT3 activation and expression of its target genes. MIC was found to inhibit the growth and migration of lung cancer cells. This finding suggests a novel pathway, where MIC suppresses survival of lung cancer cells through inactivation of STAT3 through inhibition of DDIAS-STAT3 interaction.

## 2 | MATERIALS AND METHODS

### 2.1 | Antibodies and reagents

The following antibodies were used in this study: anti-DDIAS from Atlas Antibodies; anti-HA, anti-Myc, anti-PARP, and anti-actin from Santa Cruz Biotechnology; anti-Caspase-3, anti-STAT3, anti-Flag, anti-HA, anti-pSTAT1 (Y701), anti-pAKT (S473), anti-pERK1/2 (T202/Y204), anti-pSTAT3 (Y705), anti-pSTAT3 (S727),

anti-survivin, and anti-snail from Cell Signaling Technology; anti-PTPRM from R&D systems; anti-GAPDH from AbFrontier; anti-Flag from Sigma-Aldrich; and anti-Cyclin D1 from BD Biosciences. MIC, 2-(4-aminophenyl)-1H-indole-6-carboxamide (DAPI) and sulforhodamine B were obtained from Sigma-Aldrich. 4xM67 pTATA TK-Luc, Flag-DDIAS and HA-STAT3 were cloned as previously described.<sup>16</sup>

### 2.2 | Screening of chemical libraries using yeast two-hybrid analysis

To search for drugs that inhibit DDIA/STAT3 binding, we used a yeast two-hybrid (Y2H) assay. The Y2H system was established as described previously.<sup>23</sup> DDIAS C-terminus (aa 784-998, 215 aa) was cloned into BamHI/PstI sites of the pGBKT7 vector (Clontech, USA) containing the DNA binding domain of GAL4 (GAL4DB) and TRP1 as a selection marker in yeast. STAT3 C-terminus (aa 583-770, 188 aa) was cloned into EcoRI/XhoI sites of the pGADT7 AD vector (Clontech) containing the Gal4 activation domain (GAL4AD) and LEU2 as a selection marker in yeast. These constructs were transformed into yeast AH109 strain containing three reporters (*ADE2*, *HIS3* and *lacZ*). Each of the transformed cells was grown on selection media (synthetic defined-leucine, tryptophan, alanine, histidine [SD-LWAH]) or SD-LW at 30°C for 2 days. Two protein interactions were evaluated by beta-galactosidase assay. Vectors pGBKT7 and pGADT7 were used as negative controls. We screened 11 211 chemical libraries provided by the Korea Research Institute of Chemical Technology (KRICT).

### 2.3 | Drug sensitivity test using the yeast two-hybrid assay

Chemical libraries obtained from KRICT were in the form of 20-mM stock solutions. Overnight yeast cultures were washed and then diluted to OD<sub>600</sub> = 0.25 in SD-LW or SD-LWAH medium in the presence of compounds at 20  $\mu$ M. The yeast cultures in a 384-well plate were incubated at 30°C for 2 days in duplicate. Compounds that inhibited cell growth by more than 70% in only SD-LWAH media were selected. The cultures in 96-well plates were incubated at 30°C for 2 days in duplicate. This assay was performed with 100- $\mu$ L SD-LW or SD-LWAH medium containing the desired concentration (5, 10 or 20  $\mu$ M) of the selected compounds. Growth of the cultures was analyzed by measuring the absorbance at 600 nm using EMax. The average of the two OD<sub>600</sub> readings was calculated and used for analysis.

### 2.4 | Cell culture and viability

Human embryonic kidney cells expressing the SV40 large T antigen (HEK293T), human lung fibroblasts (WI-38 and IMR-90), and non-small cell lung cancer cell lines (NCI-H23, NCI-H1703, NCI-H1793 and NCI-H2009) were purchased from the ATCC or the Korean Cell Line Bank. HEK293T, WI-38 and IMR-90 cells were cultured in DMEM, and

NCI-H23, NCI-H1703, NCI-H1793 and NCI-H2009 cells were cultured in RPMI-1640 supplemented with 10% FBS. Cells were transfected with each plasmid using Turbofect (Thermo Fisher Scientific) according to the manufacturer's instructions. Cell viability was determined using the sulforhodamine B assay as previously described.<sup>24</sup>

## 2.5 | Luciferase reporter assays

Cells were co-transfected with 300 ng of 4xM67 pTATA TK-Luc and 10 ng of pRL-TK using 1  $\mu$ L of Turbofect per well in 48-well plates and treated with MIC for 12 hours. Luciferase assay was performed as previously described.<sup>12</sup>

## 2.6 | Cell migration and invasion assay

The assays were performed in 24-well transwell plates (BD Biosciences) with 8- $\mu$ m-pore inserts coated with or without Matrigel (Invitrogen). Cells ( $1 \times 10^5$ ) treated with MIC for 12 hours were seeded in a culture insert of the upper chamber. Complete medium was applied to the lower chamber. Cells were allowed to migrate/invade the layer for 12 or 24 hours, respectively. Migrating/invading cells were stained with 0.4% SRB and visualized under a microscope.

## 2.7 | Reverse transcription and quantitative PCR

Total RNA isolated using TRIzol (Invitrogen) was reverse-transcribed into cDNA using a TOPscript RT kit (Enzymomics) according to the manufacturer's protocol. Real-time PCR was performed using cDNA with a PCR Master Mix Kit (Enzymomics) and analyzed by PCR machine Rotor-Gene 6000 (Qiagen). The primers for Cyclin D1 (P298560), Survivin (P124676) and STAT3 (P229000) were obtained from Bioneer. Primers for DDIAS, snail and GAPDH were used as described previously.<sup>13</sup> All reactions were normalized to GAPDH as an internal control.

## 2.8 | Immunocytochemistry

Immunofluorescence staining was performed as previously described.<sup>13</sup> Cells were incubated with anti-phospho-STAT3 (Y705) antibody overnight. The images were visualized using an LSM 800 fluorescence microscope (Zeiss).

## 2.9 | Co-immunoprecipitation and immunoblotting assays

Immunoprecipitation and immunoblotting were performed as described previously.<sup>15</sup> Western blot signals were detected using an enhanced chemiluminescence (ECL) kit (Millipore).

## 2.10 | Xenograft mouse model

All animal experimental protocols were approved by the bioethics committee of the Korea Research Institute of Bioscience and Biotechnology (KRIBB). NCI-H1703 ( $9 \times 10^6$ /mouse) cells were injected subcutaneously into 6-week-old female Balb/c nude mice to generate tumors (5 mice per group). When the tumors grew to 60–70 mm<sup>3</sup>, MIC was administered intraperitoneally once a day for 21 days. Tumor volumes (V) were determined using the following equation: volume (mm<sup>3</sup>) = (length  $\times$  width  $\times$  height)  $\times$  0.5.

## 2.11 | Statistical analysis

The experiments were performed in triplicate. The results are presented as means  $\pm$  SEM of at least three independent experiments. Statistical analyses were performed using a two-tailed Student's *t* test. A value of *P* < 0.05 was accepted as significant.

# 3 | RESULTS

## 3.1 | Screening and identification of an inhibitor for DNA damage-induced apoptosis suppressor/signal transducer and activator of transcription 3 binding

Although we showed the binding of DDIAS to STAT3 C-terminus (aa 583–770),<sup>16</sup> the binding region of STAT3 for DDIAS was not undetermined. First, we performed domain analysis of DDIAS to investigate the domain interacting with STAT3. Immunoprecipitation assay revealed that DDIAS C-terminus (aa 601–998) bound to STAT3 (Figure 1A). Then, the Y2H assay system was established to screen drugs to inhibit the interaction between DDIAS and STAT3. To increase the search specificity of chemicals, we wanted to use the interaction domains of DDIAS and STAT3. Previously, we found that DDIAS-CTR (aa 784–998) can be used for Y2H assay and that the other region can bind to DNA.<sup>14</sup> We also revealed that STAT3 CTR (aa 583–770) could bind to DDIAS, thereby confirming the interaction between DDIAS-CTR (aa 784–998) and STAT3 CTR (aa 583–770) (Figure S1). Y2H analysis demonstrated an interaction between DDIAS-CTR (aa 784–998) and STAT3-CTR (aa 583–770) following Ade2, His3 and LacZ reporter assays (Figure 1B). The transformed yeast cells expressing both DDIAS-CTR and STAT3-CTR grew well on the plate lacking adenine and histidine (SD-LWAH), whereas cells expressing only DDIAS-CTR or STAT3-CTR did not (Figure 1B). Similarly, cells expressing both DDIAS-CTR and STAT3-CTR also exhibited  $\beta$ -galactosidase activity, whereas negative controls did not. Western blot analysis detected protein expression of DDIAS-CTR and STAT3-CTR in the transformed yeast cells (Figure 1C). To search for drugs to inhibit DDIA/STAT3 binding, we screened 11 211 chemical libraries provided by KRIBB using the Y2H system. Of the 11 211 compounds, 24 were selected after Y2H assay. The compounds

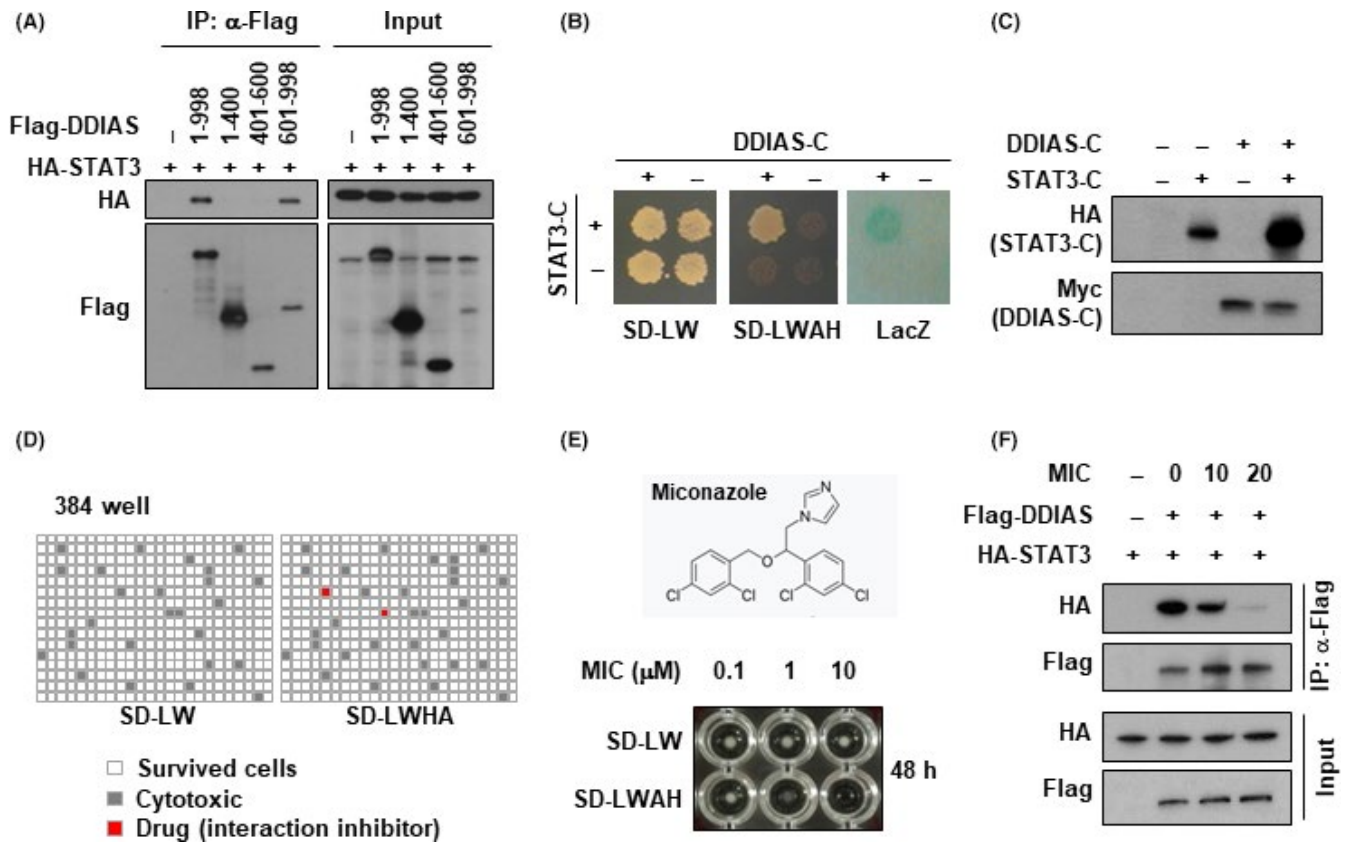


**FIGURE 1** Screening of DNA damage-induced apoptosis suppressor (DDIAS)/signal transducer and activator of transcription 3 (STAT3) inhibitors. A, Mapping of DDIAS-binding region on STAT3. Flag-DDIAS deletion constructs and HA-STAT3 were co-transfected into HEK293T cells in the indicated combinations. The cell lysates were subjected to an immunoprecipitation assay using anti-Flag-agarose, and the immunoprecipitates were probed with anti-Flag or anti-HA antibodies. B, Yeast two-hybrid analysis. Yeast cells transformed with DDIAS-C and STAT3-C were grown on the selection media (middle panel), as described in the Materials and Methods. The positive interaction between DDIAS-C and STAT3-C was confirmed by  $\beta$ -galactosidase assay (right panel). C, Expression of fusion proteins in yeast. Yeast cell lysates transformed with DDIAS-C or/and STAT3-C were subjected to western blot analysis using anti-HA or anti-Myc antibodies. D, Scheme of DDIAS/STAT3 inhibitor screening using yeast. E, Identification of miconazole as a DDIAS/STAT3 inhibitor. Yeast cells transformed with DDIAS-C and STAT3-C were grown with the indicated dose in selective media (SD-LW or SD-LWAH) for 48 h. F, Miconazole (MIC) inhibits DDIAS-STAT3 interaction. Cells were transfected with Flag-DDIAS and HA-STAT3 and incubated with either MIC (10, 20  $\mu$ mol/L) or vehicle (DMSO). Cell lysates were immunoprecipitated with flag-agarose beads and analyzed by western blotting

inhibiting cell growth in both SD-LW and SD-LWAH media were excluded, as they were generally toxic to yeast cells (Figure 1D). Eight of these selected compounds showed dose-dependent growth inhibition of yeast cells; among these, we chose MIC, which is commercially available, for further analysis. MIC suppressed the cell growth of yeast in SD-LWAH but not in SD-LW (Figure 1E). These data suggest that MIC inhibits binding between DDIAS and STAT3. Furthermore, analysis of whether Flag-DDIAS interacts with HA-STAT3 in the presence of MIC (Figure 1F) revealed that Flag-DDIAS/HA-STAT3 binding was blocked following MIC treatment.

### 3.2 | Miconazole suppresses the activation of signal transducer and activator of transcription 3

Previously, we showed that DDIAS binds to STAT3 and promotes STAT3 Y705 phosphorylation in lung cancer.<sup>16</sup> DDIAS competes

with PTPRM, a novel STAT3 phosphatase, for STAT3 binding. Because MIC was identified as an inhibitor of DDIAS-STAT3 binding, we expected that MIC would suppress STAT3 Y705 phosphorylation.

To address whether MIC suppresses STAT3 signaling, we examined the phosphorylation status of STAT3 in the presence of MIC. MIC suppressed the phosphorylation of STAT3 Y705, but not S727, in a dose-dependent manner in both NCI-H23 and NCI-H1703 cells wherein the expression levels of DDIAS and STAT3 are relatively high (Figure 2A). The phosphorylation of STAT3 was suppressed within 1 hour following MIC treatment in both NCI-H23 and NCI-H1703 cells (Figure 2B). MIC suppressed the overall phosphorylation of STAT3 in both NCI-H23 and NCI-H1703 cells in the immunocytochemical analysis (Figure 2C). However, MIC did not reduce the phosphorylation of STAT1, AKT or ERK1/2 (Figure 2D). These results support the ability of MIC to inhibit STAT3 tyrosine phosphorylation.



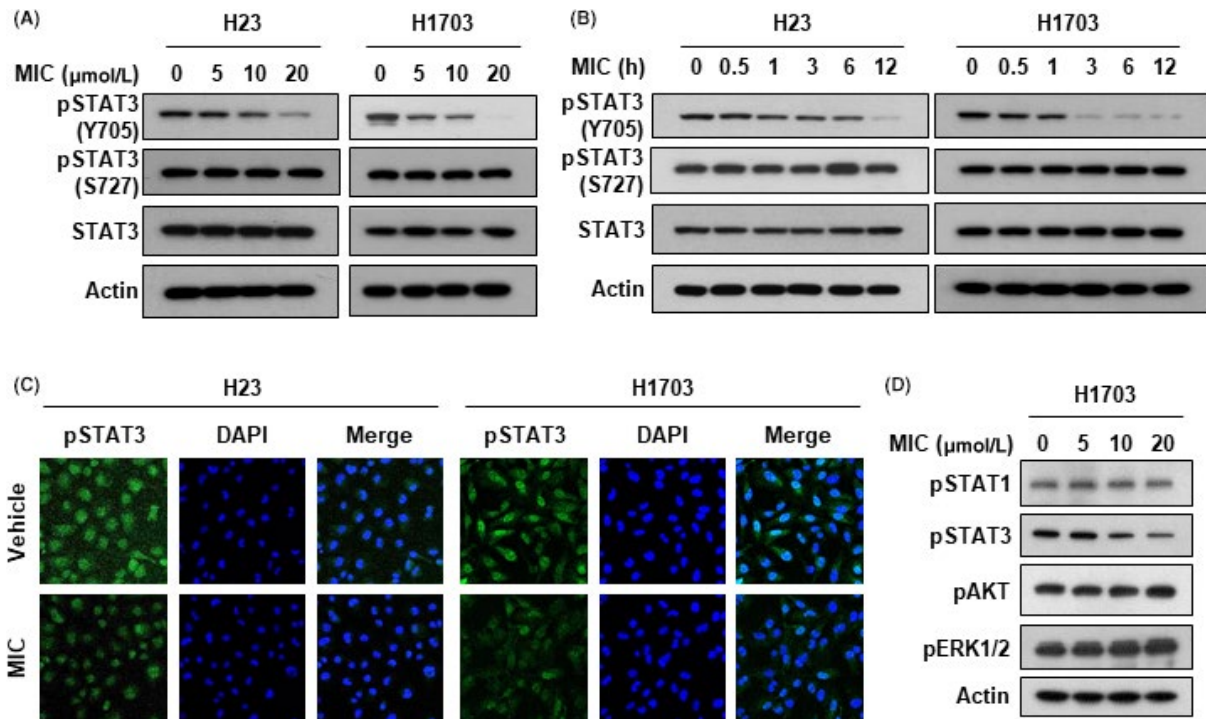


**FIGURE 2** Miconazole (MIC) specifically suppresses the STAT3 signaling pathway. A, Signal transducer and activator of transcription 3 (STAT3) phosphorylation in NCI-H23 and NCI-H1703 cells treated with MIC for 3 h. B, STAT3 phosphorylation in cells treated with MIC (10  $\mu\text{mol/L}$ ) for indicated times. C, Immunocytochemistry of cells treated with MIC (10  $\mu\text{mol/L}$ ) for 3 h. D, Effects of MIC on other kinases in NCI-H1703 cells treated with MIC for 3 h

### 3.3 | Miconazole suppresses the expression of signal transducer and activator of transcription 3 target genes through inhibiting DNA damage-induced apoptosis suppressor-signal transducer and activator of transcription 3 binding

To determine whether MIC regulates the expression of STAT3 target genes, we performed a luciferase assay using a reporter gene (M67-Luc) containing STAT3 binding sites in lung cancer cells. MIC suppressed STAT3 luciferase activity in a dose-dependent manner (Figure 3A). Then, we examined the mRNA levels of STAT3 target genes, cyclin D1, snail and survivin in the MIC-treated cells. MIC suppressed the mRNA level of cyclin D1, snail and survivin. However, MIC did not show any influence on the expression of STAT3 or DDIAS itself (Figure 3B). Moreover, western blot analysis revealed that MIC decreased the protein level of cyclin D1, snail and survivin in MIC-treated lung cancer cells (Figure 3C). This result suggests that MIC suppresses the expression of STAT3 target genes through inactivating STAT3 by blocking DDIAS-STAT3 interaction.

### 3.4 | Miconazole inhibits cell growth and migration of lung cancer

We found that the expression levels of STAT3 and DDIAS were low in normal human lung fibroblast cells, WI-38 or IMR-90,

compared with those in non-small-cell lung carcinoma (NSCLC), such as NCI-H23 or NCI-H1703 cells (Figure 4A). To test whether MIC inhibits growth and migration of lung cancer cells, we examined the effect of MIC in WI-38, NCI-H1703, NCI-H1793 and NCI-H2009. MIC inhibited the cell growth of NSCLC but not WI-38 (Figure 4B). Moreover, MIC treatment increased Annexin V-stained cells, indicating apoptotic cell death in NCI-H23 or NCI-H1703 (Figure 4C). As expected, western blot analysis showed the cleavage of PARP and caspase-3 in the cells treated with MIC (Figure 4D). Furthermore, MIC significantly suppressed migration and invasion of NSCLC (Figure 4E,F). These results suggest that MIC suppressed cell growth, migration and invasion of NSCLC.

### 3.5 | Miconazole inhibits tumor growth using mouse xenograft

To investigate the effect of MIC on tumor growth, we carried out a xenograft assay using the NCI-H1703 mouse model. MIC (50 mg/kg) was administered to mice via intraperitoneal injection. Mice that received MIC showed no significant change in body weight (Figure 5A). Tumor growth was suppressed by 42.7% in MIC-treated mice compared with that in vehicle-treated mice (Figure 5B,C). Western blot analysis showed decreased phosphorylation of STAT3 in MIC-treated tumor tissues compared with that in vehicle-treated tumor tissues (Figure 5D). As expected,

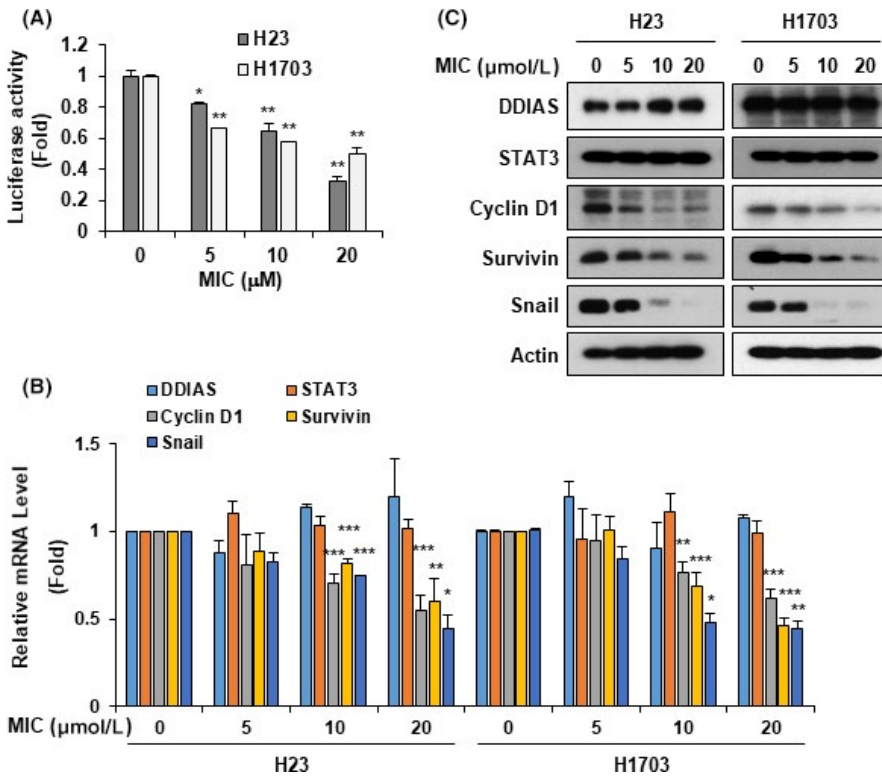


**FIGURE 3** Miconazole (MIC) suppresses the expression of STAT3 targets by disrupting the interaction between DNA damage-induced apoptosis suppressor (DDIAS) and signal transducer and activator of transcription 3 (STAT3). A, Inhibition of STAT3 transactivation by MIC. NCI-H23 and NCI-H1703 cells were transfected with M67-Luc and TK-Ren for 36 h and treated with MIC for 12 h. Relative luciferase activity is shown. B, Expression of DDIAS, STAT3 and STAT3 target genes, as determined by real-time quantitative PCR performed 24 h after MIC treatment. C, Protein level of STAT3 targets, as determined by western blot analyses performed 24 h after MIC treatment. All experiments were performed in triplicate three times. The values represent means  $\pm$  SEM. \*  $P < 0.05$ , \*\*  $P < 0.01$ , \*\*\*  $P < 0.001$

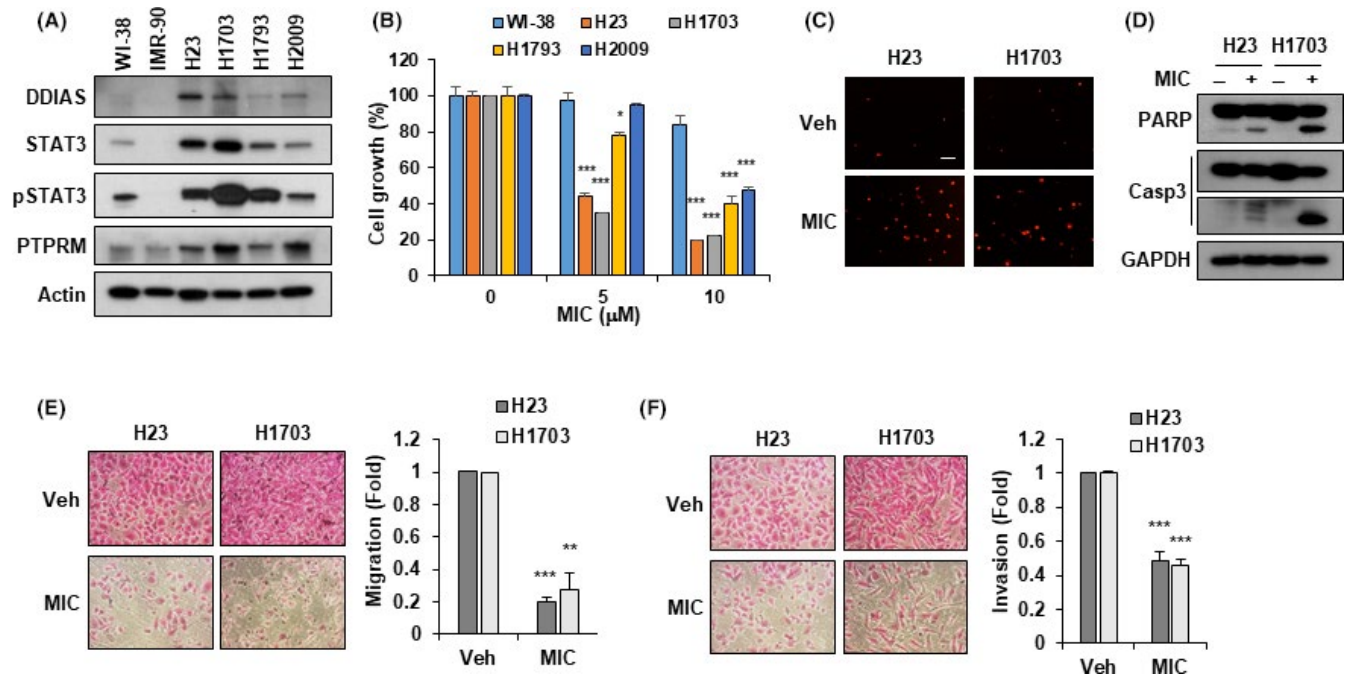
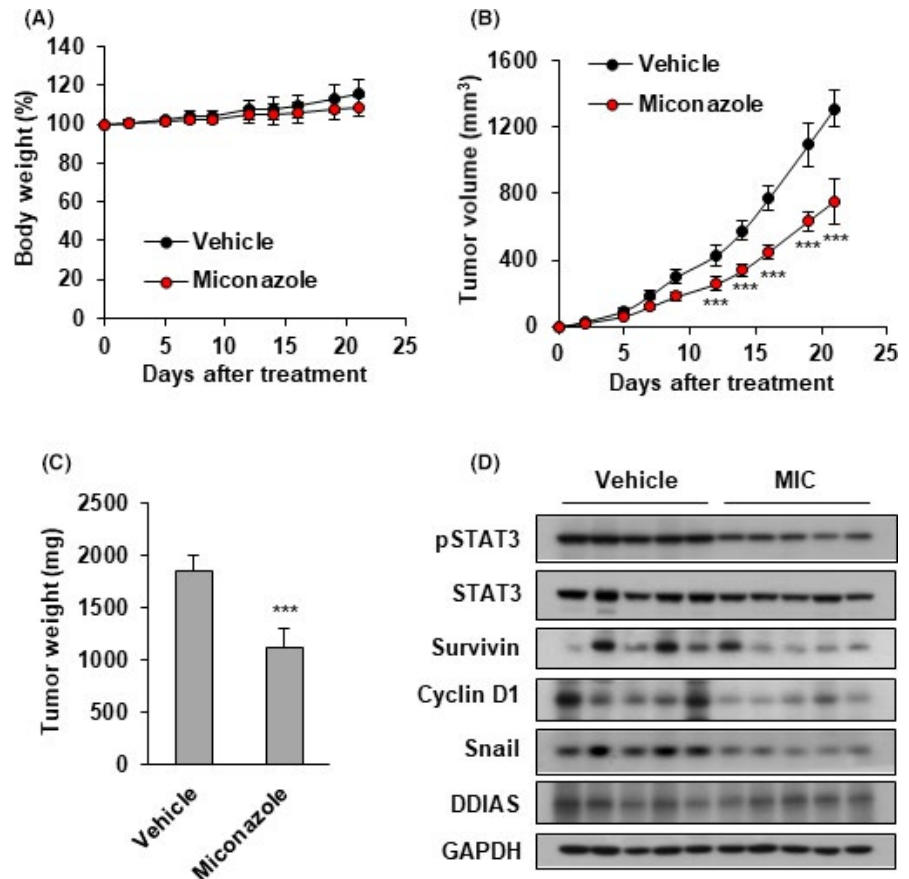


**FIGURE 4** Miconazole (MIC) inhibits cell growth, migration and invasion of lung cancer. A, Western blot analysis in human normal lung fibroblast cells (WI-38 and IMR-90) and non-small-cell lung carcinoma (NSCLC) (H23, H1703, H1793 and H2009). B, Cell growth of WI-38, H23, H1703, H1793 or H2009 cells determined by SRB assay following culturing for 72 h after MIC treatment. C, Annexin V staining of cells treated with MIC (10  $\mu\text{mol/L}$ ) for 72 h. D, Western blot analysis of cells treated with MIC (10  $\mu\text{mol/L}$ ) for 72 h. E, Migration assay of cells treated with MIC for 12 h. F, Invasion assay of cells treated with MIC for 24 h. The values represent means  $\pm$  SEM. \*\* $P < 0.01$ , \*\*\* $P < 0.001$

expression levels of STAT3 target genes, cyclin D1, survivin and snail were reduced in tumor tissues obtained from MIC-treated mice, whereas those of STAT3 and DDIAS were not (Figure 5D).

This result implies that MIC inhibits tumor growth by reducing the phosphorylation of STAT3 and the expression of its targets in an in vivo xenograft assay.

**FIGURE 5** Miconazole (MIC) reduces the growth of tumor xenograft in nude mice inoculated with NCI-H1703 xenografts. MIC (50 mg/kg) was intraperitoneally injected into each mouse. A, Body weight. (n = 5 per group). B, Tumor volume. C, Tumor weight. D, Western blot analysis revealing suppression of signal transducer and activator of transcription 3 (STAT3) activation and its targets by MIC. The values represent means  $\pm$  SEM. \*\*\*  $P < 0.001$



## 4 | DISCUSSION

Persistent STAT3 activation is a significant biomarker of malignant human cancers.<sup>8,9</sup> Targeting STAT3 is a valid therapeutic approach for anti-cancer drug design, and numerous strategies have been developed. First, it is considered that blocking the interaction between STAT3 and other proteins promotes the STAT3 signaling pathway. Small molecule inhibitors, such as cell surface receptor inhibitors or kinase inhibitors, are developed by targeting the upstream of STAT3.<sup>25,26</sup> Among them, JAK or Src inhibitors have been widely developed and are currently in clinical trials. However, these approaches are limited by off-target toxicity. Several JAK/Src inhibitors have limitations as cancer therapeutic agents due to on-target toxicity that induces inflammation related to other member of the STAT family.

Different inhibitors directly targeting STAT3 have recently emerged. These inhibitors act through three distinct approaches to inhibit the DNA binding domain (DBD), the N-terminal domain and the SH2 domain of STAT3. Research on developing STAT3 inhibitors has focused on targeting its SH2 domain and blocking its dimerization, as the dimerization of STAT3 via an SH2 domain is crucial for its activation.<sup>27-29</sup> Several inhibitors targeting the SH2 domain of STAT3, such as Stattic, STA-21 and S3I-201, have been developed and reported using virtual screening and other methods.<sup>28-30</sup> BP-1-102, an analog of S3I-201.1066, binds to STAT3 pY705 or gp130 pY904 and competes with STAT3 pY705 or gp130 pY904, resulting

in the suppression of the STAT3 signaling pathway.<sup>27</sup> However, none of these inhibitors has reached the clinic for cancer therapy.

Our previous report suggested that DDIAS is a positive regulator of STAT3 and promotes STAT3 tyrosine phosphorylation through inhibition of PTPRM recruitment.<sup>16</sup> DDIAS interacts with STAT3 and competes with PTPRM. Based on our previous data, the evidence that the DDIAS protein level correlates strongly with STAT3 activation in human lung cancer tissues supports these hypotheses. In this study, we propose the DDIAS/STAT3 pathway as a therapeutic target. DDIAS expression is relatively low in normal lung fibroblasts but very high in human lung cancer cell lines and tumor tissues, in which STAT3 is phosphorylated at Y705.<sup>16</sup> The interaction between DDIAS and STAT3 promotes the growth and migration of lung cancer (Figure 6A). We screened and identified an inhibitor of DDIAS/STAT3 binding using the Y2H system. MIC inhibited the interaction of DDIAS with STAT3 and only STAT3 Y705 phosphorylation (Figure 6B). Consequently, MIC represses cell growth and migration of lung cancer through inhibiting the expression of STAT3 target genes. We suggest that the TAD domain of STAT3 containing tyrosine 705 is the binding region for DDIAS. To investigate the binding site of STAT3 for interaction with DDIAS, we performed an immunoprecipitation assay using SH2 or TAD domain-deleted mutant of STAT3. Only the mutant with deleted TAD domain of STAT3 hampered DDIAS/STAT3 binding (Figure S2). Therefore, our data suggest that STAT3 TAD domain functions as the binding site for DDIAS. MIC combined with a known STAT3 inhibitor, STA-21, targeting the

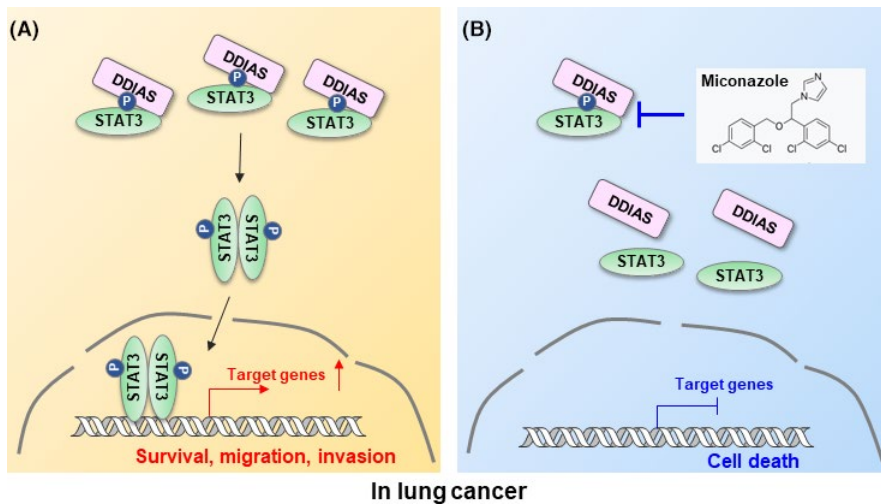


**FIGURE 6** Schematic model of miconazole (MIC) anti-tumor activity via inhibition of DNA damage-induced apoptosis suppressor (DDIAS)/signal transducer and activator of transcription 3 (STAT3). A. DDIAS/STAT3 interaction promotes the growth and migration of lung cancer. B. MIC inhibited DDIAS/STAT3 interaction and STAT3 Y705 phosphorylation, repressing cell growth

SH domain of STAT3, exerted an additive effect on cell growth inhibition (Figure S3).

Miconazole is an antifungal reagent. MIC possesses anti-tumor activity by multiple pathways in various human cancers. MIC induces p53-dependent apoptosis in human colon carcinoma,<sup>19</sup> and bladder cancer cell death via the death receptor 5-dependent and mitochondrial-mediated pathways.<sup>21</sup> MIC suppresses p70S6K phosphorylation through inhibiting mTOR signaling.<sup>20</sup>

Our data demonstrate a novel mechanism for the anti-tumor activity of MIC in human lung cancer cells and provide evidence supporting the potential of MIC as a therapeutic agent against cancer. We propose, for the first time, that MIC suppresses STAT3 tyrosine phosphorylation, thereby inhibiting the STAT3 signaling pathway. Importantly, tyrosine phosphorylation of STAT1 was not reduced by MIC, and STAT5 phosphorylation was not detected in NCI-H1703 used in this study (data not shown). The specificity of MIC toward inhibition of STAT3 is valuable for cancer therapy. Moreover, MIC as a DDIAS/STAT3 inhibitor suppresses STAT3 tyrosine 705 phosphorylation but not serine 727 phosphorylation. These data support our previous report that DDIAS promotes STAT3 tyrosine phosphorylation, resulting from inhibiting PTPRM recruitment to STAT3 through the interaction with STAT3.<sup>16</sup> In light of the fact that MIC exhibits little effect on the activation of STAT1 as well as other kinases such as AKT or ERK1/2, we suggest that MIC regulates the DDIAS-mediated STAT3 pathway. It remains unclear whether MIC directly binds to STAT3 or DDIAS. MIC itself does not suppress the expression of DDIAS and STAT3. In this regard, it is informative to examine the status of beta-catenin in the MIC-treated cells, because DDIAS is known as a positive regulator of beta-catenin stability. Western blot analysis showed that MIC did not change the expression of beta-catenin protein levels at the time pSTAT3 (Y705) decreased (Figure 4A). Although DDIAS knockdown induced the degradation of beta-catenin protein,<sup>13</sup> we did not determine that DDIAS regulates beta-catenin stability through their direct binding. Immunoprecipitation assay revealed that DDIAS did not interact with beta-catenin (Figure 4B). Our data indicated that

DDIAS regulated protein levels of beta-catenin regardless of its direct binding to it. Therefore, it is likely that MIC binds to DDIAS. If MIC binds to STAT3 and thereby inhibits the interaction with DDIAS as well as the interaction with PTPRM, the level of phospho-STAT3 would be expected to remain unchanged.

In conclusion, we report here that MIC is a novel inhibitor of the DDIAS/STAT3 pathway in lung cancer cells, providing valuable information for the development of novel therapeutic agents for the prevention and treatment of cancer.

#### ACKNOWLEDGMENT

We thank Min Jeong Ahn and Gyuri Kim for technical assistance. This work was supported by the KRIBB Initiative Program (KGM4751713) and the National Research Foundation (NRF) (NRF-2015M3A9A8032460, NRF-2017R1A2B2011936 and NRF-2017M3A9F9030565).

#### CONFLICT OF INTEREST

The authors have no conflict of interest.

#### ORCID

Joo-Young Im  <https://orcid.org/0000-0001-6923-8189>

Misun Won  <https://orcid.org/0000-0001-6626-0647>

#### REFERENCES

- Zhong Z, Wen Z, Darnell JE Jr. Stat3: a STAT family member activated by tyrosine phosphorylation in response to epidermal growth factor and interleukin-6. *Science*. 1994;264:95-98.
- Akira S, Nishio Y, Inoue M, et al. Molecular cloning of APRF, a novel IFN-stimulated gene factor 3 p91-related transcription factor involved in the gp130-mediated signaling pathway. *Cell*. 1994;77:63-71.
- Darnell JE Jr, Kerr IM, Stark GR. Jak-STAT pathways and transcriptional activation in response to IFNs and other extracellular signaling proteins. *Science*. 1994;264:1415-1421.
- Beadling C, Guschin D, Witthuhn BA, et al. Activation of JAK kinases and STAT proteins by interleukin-2 and interferon alpha, but not the T cell antigen receptor, in human T lymphocytes. *EMBO J*. 1994;13:5605-5615.



5. Schindler C, Shuai K, Prezioso VR, Darnell JE Jr. Interferon-dependent tyrosine phosphorylation of a latent cytoplasmic transcription factor. *Science*. 1992;257:809-813.
6. Takeda K, Akira S. STAT family of transcription factors in cytokine-mediated biological responses. *Cytokine Growth Factor Rev*. 2000;11:199-207.
7. Schindler C, Darnell JE Jr. Transcriptional responses to polypeptide ligands: the JAK-STAT pathway. *Annu Rev Biochem*. 1995;64:621-651.
8. Yu H, Jove R. The STATs of cancer—new molecular targets come of age. *Nat Rev Cancer*. 2004;4:97-105.
9. Yu H, Pardoll D, Jove R. STATs in cancer inflammation and immunity: a leading role for STAT3. *Nat Rev Cancer*. 2009;9:798-809.
10. Won KJ, Im JY, Yun CO, et al. Human Noxin is an anti-apoptotic protein in response to DNA damage of A549 non-small cell lung carcinoma. *Int J Cancer*. 2014;134:2595-2604.
11. Zhang ZZ, Huang J, Wang YP, Cai B, Han ZG. NOXIN as a cofactor of DNA polymerase-primase complex could promote hepatocellular carcinoma. *Int J Cancer*. 2015;137:765-775.
12. Im JY, Lee KW, Won KJ, et al. DNA damage-induced apoptosis suppressor (DDIAS), a novel target of NFATc1, is associated with cisplatin resistance in lung cancer. *Biochim Biophys Acta*. 2016;1863:40-49.
13. Im JY, Yoon SH, Kim BK, et al. DNA damage induced apoptosis suppressor (DDIAS) is upregulated via ERK5/MEF2B signaling and promotes beta-catenin-mediated invasion. *Biochim Biophys Acta*. 2016;1859:1449-1458.
14. Won KJ, Im JY, Kim BK, et al. Stability of the cancer target DDIAS is regulated by the CHIP/HSP70 pathway in lung cancer cells. *Cell Death Dis*. 2017;8:e2554.
15. Im JY, Kim BK, Lee JY, et al. DDIAS suppresses TRAIL-mediated apoptosis by inhibiting DISC formation and destabilizing caspase-8 in cancer cells. *Oncogene*. 2018;37:1251-1262.
16. Im JY, Kim BK, Lee KW, Chun SY, Kang MJ, Won M. DDIAS promotes STAT3 activation by preventing STAT3 recruitment to PTPRM in lung cancer cells. *Oncogenesis*. 2020;9:1.
17. Ayub M, Levell MJ. The inhibition of human prostatic aromatase activity by imidazole drugs including ketoconazole and 4-hydroxyandrostenedione. *Biochem Pharmacol*. 1990;40:1569-1575.
18. Kobayashi D, Kondo K, Uehara N, et al. Endogenous reactive oxygen species is an important mediator of miconazole antifungal effect. *Antimicrob Agents Chemother*. 2002;46:3113-3117.
19. Wu CH, Jeng JH, Wang YJ, et al. Antitumor effects of miconazole on human colon carcinoma xenografts in nude mice through induction of apoptosis and G0/G1 cell cycle arrest. *Toxicol Appl Pharmacol*. 2002;180:22-35.
20. Park JY, Jung HJ, Seo I, et al. Translational suppression of HIF-1alpha by miconazole through the mTOR signaling pathway. *Cell Oncol*. 2014;37:269-279.
21. Yuan SY, Shiau MY, Ou YC, et al. Miconazole induces apoptosis via the death receptor 5-dependent and mitochondrial-mediated pathways in human bladder cancer cells. *Oncol Rep*. 2017;37:3606-3616.
22. Chang HT, Chen WC, Chen JS, et al. Effect of miconazole on intracellular Ca<sup>2+</sup> levels and proliferation in human osteosarcoma cells. *Life Sci*. 2005;76:2091-2101.
23. Kim DM, Chung KS, Choi SJ, et al. RhoB induces apoptosis via direct interaction with TNFAIP1 in HeLa cells. *Int J Cancer*. 2009;125:2520-2527.
24. Vichai V, Kirtikara K. Sulforhodamine B colorimetric assay for cytotoxicity screening. *Nat Protoc*. 2006;1:1112-1116.
25. Furtek SL, Backos DS, Matheson CJ, Reigan P. Strategies and approaches of targeting STAT3 for cancer treatment. *ACS Chem Biol*. 2016;11:308-318.
26. Kim BH, Yi EH, Ye SK. Signal transducer and activator of transcription 3 as a therapeutic target for cancer and the tumor microenvironment. *Arch Pharm Res*. 2016;39:1085-1099.
27. Zhang X, Yue P, Page BD, et al. Orally bioavailable small-molecule inhibitor of transcription factor Stat3 regresses human breast and lung cancer xenografts. *Proc Natl Acad Sci USA*. 2012;109:9623-9628.
28. Song H, Wang R, Wang S, Lin J. A low-molecular-weight compound discovered through virtual database screening inhibits Stat3 function in breast cancer cells. *Proc Natl Acad Sci USA*. 2005;102:4700-4705.
29. Siddiquee K, Zhang S, Guida WC, et al. Selective chemical probe inhibitor of Stat3, identified through structure-based virtual screening, induces antitumor activity. *Proc Natl Acad Sci USA*. 2007;104:7391-7396.
30. Schust J, Sperl B, Hollis A, Mayer TU, Berg T. Stattic: a small-molecule inhibitor of STAT3 activation and dimerization. *Chem Biol*. 2006;13:1235-1242.

## SUPPORTING INFORMATION

Additional supporting information may be found online in the Supporting Information section.

**How to cite this article:** Yoon S-H, Kim B-K, Kang M-J, Im J-Y, Won M. Miconazole inhibits signal transducer and activator of transcription 3 signaling by preventing its interaction with DNA damage-induced apoptosis suppressor. *Cancer Sci*. 2020;111:2499-2507. <https://doi.org/10.1111/cas.14432>